

Validation of an Equilibrium-Stage Model of the Coldfinger Water Exhauster for Enhanced Glycol Regeneration in Natural Gas Dehydration

Andreasen, Anders; Romero, Iveth; Maschietti, Marco

Published in:
Industrial and Engineering Chemistry Research

DOI (link to publication from Publisher):
[10.1021/acs.iecr.0c03292](https://doi.org/10.1021/acs.iecr.0c03292)

Publication date:
2020

Document Version
Accepted author manuscript, peer reviewed version

[Link to publication from Aalborg University](#)

Citation for published version (APA):
Andreasen, A., Romero, I., & Maschietti, M. (2020). Validation of an Equilibrium-Stage Model of the Coldfinger Water Exhauster for Enhanced Glycol Regeneration in Natural Gas Dehydration. *Industrial and Engineering Chemistry Research*, 59(44), 19668-19679. <https://doi.org/10.1021/acs.iecr.0c03292>

General rights

Copyright and moral rights for the publications made accessible in the public portal are retained by the authors and/or other copyright owners and it is a condition of accessing publications that users recognise and abide by the legal requirements associated with these rights.

- Users may download and print one copy of any publication from the public portal for the purpose of private study or research.
- You may not further distribute the material or use it for any profit-making activity or commercial gain
- You may freely distribute the URL identifying the publication in the public portal -

Take down policy

If you believe that this document breaches copyright please contact us at vbn@aub.aau.dk providing details, and we will remove access to the work immediately and investigate your claim.

1 **Validation of an Equilibrium-Stage Model of the Coldfinger Water Exhauster for**
2 **Enhanced Glycol Regeneration in Natural Gas Dehydration**

3 Anders Andreasen^a, Iveth Romero^b, Marco Maschietti^{b*}

4 ^aRamboll Energy, Field Development, Studies and FEED, Bavneshøjvej 5, 6700 Esbjerg, Denmark.
5

6 ^bAalborg University, Department of Chemistry and Bioscience, Niels Bohrs Vej 8A, 6700, Esbjerg,
7 Denmark
8

9 * E-mail: marco@bio.aau.dk
10
11
12
13
14
15
16
17
18
19

Accepted author manuscript

20 **Abstract**

21 A model of the Coldfinger water exhauster for advanced glycol regeneration, based on two-equilibrium
22 stages with internal recirculation of vapor, is proposed and validated on plant data of natural gas
23 dehydration using triethylene glycol (TEG). Optimal operating regions are located for vapor
24 recirculation ratios (α) above 0.95, gas-to-liquid feed ratios in the order of 10^{-4} and top temperatures in
25 the range 50 to 80 °C. The conceptual investigation supports that the Coldfinger unit can enhance TEG
26 purity up to approximately 99.7 wt %. Taking conventional single-stage gas stripping as reference, the
27 model supports the possibility of achieving the same TEG enrichment levels using 10 to 100 times less
28 gas. Non-obvious features are also highlighted, such as multiple steady-states and conditions leading to
29 low or negative efficiency. The model provides a good fit with plant data with optimal values of α
30 (regression parameter) being consistent and bearing sound physical meaning.

31

32

1. Introduction

Gas dehydration is one of the conditioning processes applied to set natural gas to optimal conditions for transport or sales. The aim of gas dehydration is to lower the content of water normally present in a produced gas stream in order to avoid hydrate formation or corrosion in the processing facilities, flow lines and pipelines. Among gas dehydration processes, water removal through absorption with triethylene glycol (TEG) is widely applied in the gas industry.¹ The process specification for the water content in the dry gas is typically set in the range 4 to 7 lb/MMSCF,² which corresponds to mole fractions from $8.4 \cdot 10^{-5}$ to $1.5 \cdot 10^{-4}$.

The process flow diagram of a basic gas dehydration unit with TEG is presented in Figure 1. In the absorption column (the absorber), water is removed from the gas stream by countercurrent contact with

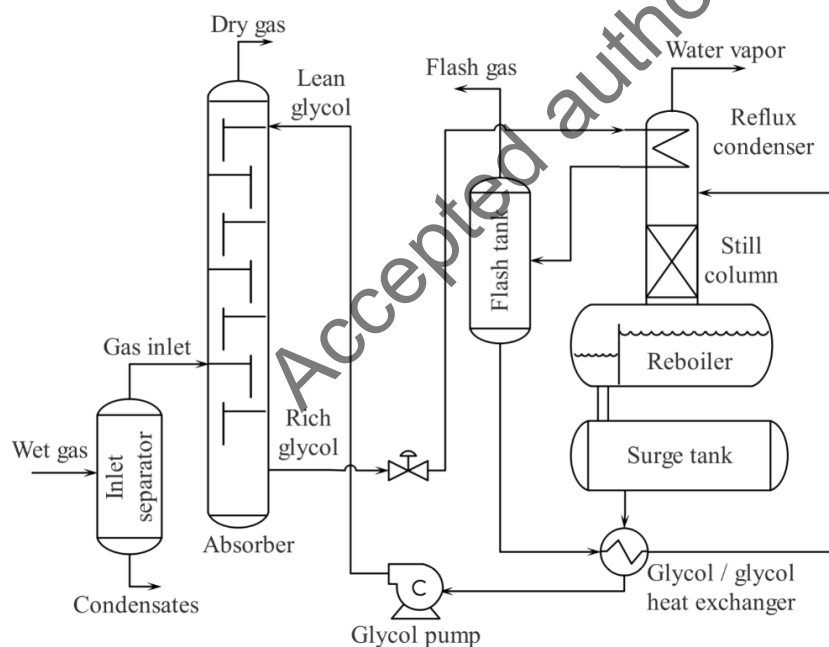


Figure 1. Process flow diagram of a typical basic gas dehydration unit with glycol.

45 TEG (lean glycol). The absorber operates under pressure with the value typically being determined by
46 the available pressure of the gas feed. As a matter of fact, the achieved level of dehydration depends
47 scarcely on the operating pressure, being by far more important the purity level of TEG fed to the
48 absorber.¹ Upon absorption, the wet TEG (rich glycol in Fig. 1) is regenerated in the still column (or
49 regenerator), which operates at lower pressure and higher temperature. In the still column, the water
50 absorbed from the wet gas stream is removed by distillation, thus re-concentrating the glycol for its re-
51 use in the absorption process. It is well known that TEG mass fractions around 98.7-99.0 wt % are
52 achieved when the regenerator operates at atmospheric pressure with reboiler temperature of around
53 204 °C.¹ Normally, the temperature of the reboiler is limited to 204 °C in order to avoid TEG
54 decomposition, generally reported as possible above 200 °C and, more specifically, at around 207 °C.¹
55 As the temperature of the reboiler cannot be increased further, TEG purities around 99.0 wt % are
56 considered to be the maximum attainable levels for atmospheric distillation. However, at the current
57 levels of water content typically specified in the dry gas stream, the dehydration process requires TEG
58 at mass fractions well above 99.0 wt %. For this reason, in the last decades a great deal of attention has
59 been devoted to developing enhanced TEG re-concentration processes aiming at increasing TEG mass
60 fractions in a simple and economic way.³ The most common methods for enhancing TEG purity in the
61 regeneration section consist in the integration of additional units to the still column, which are based on
62 gas stripping (either using an inert gas or a portion of the dry gas),⁴⁻⁶ stripping using volatile
63 hydrocarbons (as in the DRIZO process),^{7,8} and Coldfinger technology.^{9,10}
64 Among enhanced TEG regeneration processes in use in the oil and gas industry, the integration of the
65 Coldfinger water exhauster into the basic process scheme is one of the preferred methods.³ In the
66 original patent disclosure,¹¹ the Coldfinger water exhauster is described as an apparatus able to further

dry the TEG-rich stream coming from a distillation unit without further increasing the temperature of said stream and without necessarily reducing pressure or using stripping gas. In a subsequent related patent disclosure,¹² the Coldfinger technology is also described as particularly suitable for offshore oil and gas installations, where space and weight limitations are important.

A typical natural gas dehydration process with an integrated Coldfinger unit is represented in Figure 2. The water exhauster, also known as Coldfinger condenser, basically consists of a cooling tube bundle (i.e. the cold finger) placed in the vapor space of a vessel fed by the liquid TEG mixture leaving the reboiler of the regenerator. Such vessel can be either an integrated section of the reboiler itself or a separate piece of equipment, such as the surge tank of Figure 2. The cooling fluid flowing inside the cooling tube bundle of the Coldfinger is generally the rich TEG coming from the absorber, albeit an

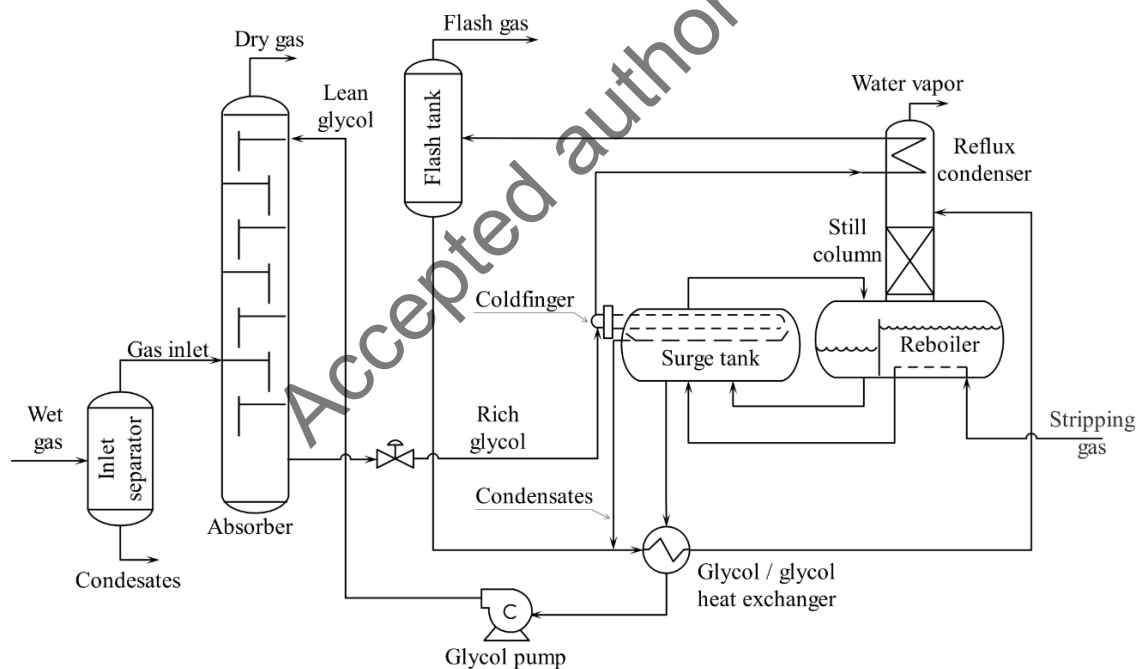


Figure 2. Process flow diagram of a typical natural gas dehydration process with the integrated Coldfinger water exhauster in the enhanced TEG regeneration section.

external source of cold water may also be used. A collection tray is placed under the cooling tube bundle for collecting the condensate, which is recirculated to the still column. The condensate removed from the exhauster is relatively richer in water. In this way, TEG is further dehydrated by continuous vaporization along with partial condensation and removal of the water-rich condensate at the top of the equipment.

The use of the Coldfinger technology is reported to allow reaching lean TEG concentrations around 99.2-99.5 wt %, even though values up to 99.7 wt %¹¹ and 99.8 wt %¹² are reported in operational examples of the related patents. Moreover, the Coldfinger water exhauster is generally considered easy to install and to integrate into TEG regeneration units³ and not requiring the use of stripping gas.^{1,3,11,12} Even though stripping gas in the water exhauster is apparently not required, typical industrial configurations of the Coldfinger may include a line for injection of dry gas or an integrated stripping column installed at the bottom of the vessel, as in the work presented by Rahimpour et al.¹³

In the recent literature review by Kong et al.,³ which includes a comparative assessment of the technologies available for advanced regeneration of TEG, the Coldfinger process is ranked as one of the best available alternatives, owing to its low capital cost and reduced revamping required for existing units. However, the lack of extensive studies on this technology is mentioned as an important drawback. More specifically, the lack of the Coldfinger unit in commercial steady-state simulation software is reported and the need for further studies focusing on how to simulate this unit is highlighted.³

It is also the opinion of the authors of this work that the lack of established modeling procedures for the Coldfinger process limits the possibility of developing sound comparisons of alternative TEG advanced regeneration technologies by professionals dealing with case studies in natural gas dehydration. As a

102 matter of fact, since the Coldfinger patent disclosures^{11,12} only a few research works have focused on
103 modeling the Coldfinger water exhauster and on developing simulation procedures of the TEG
104 regeneration process based on the Coldfinger apparatus.^{9,10,13-15} In the work of Rahimpour et al.,¹³ a
105 model based on mass and heat transfer is presented and linked to a steady-state simulation software
106 with results being compared to field data as further discussed in Section 3. In the other works,^{9,10,14,15}
107 ideal-stage based models are applied, representing the Coldfinger process as a two-stage separation
108 process with internal recirculation of the uncondensed vapor and phase equilibrium conditions assumed
109 in each stage. However, in these works^{9,10,14,15} comparisons of the results to neither field nor laboratory
110 data are presented. In addition, in most of these works^{9,10,14} indications on how to fix the two-stage
111 process model parameters (e.g. the rate of internal recirculation) in order to match the Coldfinger
112 behavior are not provided. Furthermore, an analysis on how the parameters characterizing the
113 Coldfinger water exhauster influence the process outcome is also lacking, with the exception of a plot
114 showing the influence of the rate of heat removal in the vapor section of the apparatus on the achieved
115 TEG purity.⁹

116 The recent work of Romero et al.¹⁵ presents an extensive analysis of the main process variables
117 determining the Coldfinger performance, concluding that the internal recirculation of the uncondensed
118 vapor, the injection of relatively small amounts of stripping gas to the bottom of the water exhauster
119 and the temperature at the top of the vessel (lower than the bottom temperature due to the cooling tube
120 bundle) are the main factors that strongly influence the efficiency of the Coldfinger water exhauster. In
121 addition, the work of Romero et al.¹⁵ indicates that a modeling approach based on two phase-
122 equilibrium stages connected by internal vapor recirculation can reproduce the typical TEG enrichment
123 data reported in technical and scientific literature. Nevertheless, the abovementioned work¹⁵ is based on

two approximations: (i) the Coldfinger water exhauster is fed by a simplified ternary system of CH₄-H₂O-TEG; and (ii) the internal recirculation of the vapor, the injection of stripping gas in the liquid section of the exhauster and the temperature at the top of the vessel are considered as independent variables, without imposing constraints arising from the need of matching the heat power removal and the temperature difference between the condensing vapor at the top of the equipment and the cooling fluid. In particular, the second approximation may lead to optimistic results, as energy conservation at the heat exchanger in the vapor space may be violated. In addition, the work of Romero et al.¹⁵ does not provide any comparison of the modeling results vs. literature data.

In the light of the above, the purpose of this work is to further advance the analysis presented by Romero et al.¹⁵ and to validate the model approach based on two-stage phase equilibrium with internal vapor recirculation. In addition, this work also aims at providing indications on how to set the model parameters to realistic values in order to match the behavior of the Coldfinger water exhauster, as well as to analyze the response of the equipment performance upon variations of said parameters. The analysis includes the effect of the internal recirculation of the vapor, the injected stripping gas, the heat power removal and the temperature at the cooling tube bundle. In addition, the hydrocarbon part of the feed is considered as a multicomponent system (i.e. not CH₄ only), considering a realistic natural gas stream. Furthermore, the proposed methodology of analysis is evaluated integrating the Coldfinger water exhauster model into a natural gas dehydration process simulation scheme and the results are compared to real plant data, including patent data,¹² and the plant data that was recently made available in the literature by Rahimpour et al.¹³

2. Coldfinger Modeling

The work of Romero et al.¹⁵ presents an approach for modeling the Coldfinger water exhauster as a two-stage phase equilibrium unit based on the configuration shown in Figure 3. Liquid TEG from the reboiler of the still column enters the water exhauster as a water-saturated liquid, at a purity around 98.7-99.0 wt %, under reboiler conditions of 204 °C and atmospheric pressure.¹ Since the bottom section of the Coldfinger unit operates practically at the same pressure and temperature as the reboiler of the still column,¹ a change in the overall system composition is necessary to shift the equilibrium conditions and to obtain TEG at higher purity levels. This can be achieved by injecting small quantities of dry gas and by recirculation of the uncondensed gas and vapors from the top to the bottom of the equipment. The Coldfinger internal recirculation can be driven by natural convection due to the temperature difference between the bottom (T_1) and the top section (T_2) of the vessel, with the top section operating at a lower temperature due to the heat removal. In the conceptualization scheme

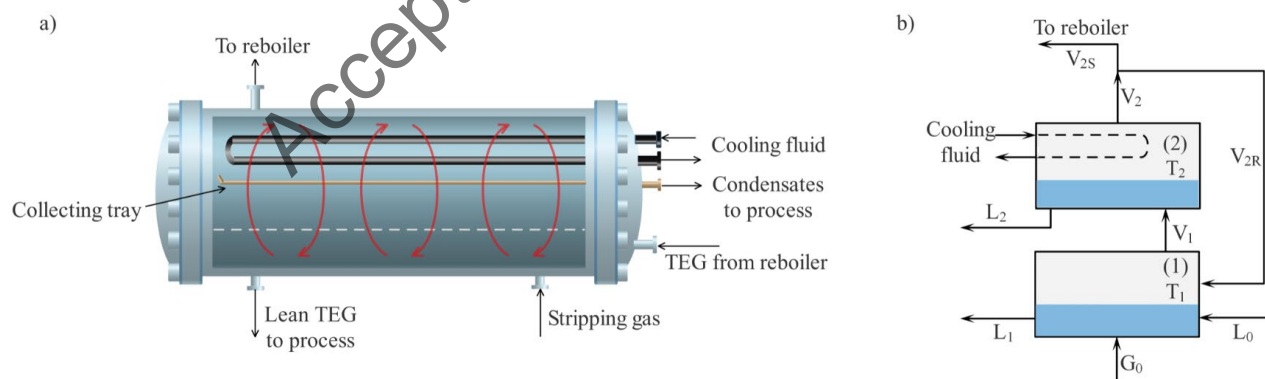


Figure 3. Schematic representation of the Coldfinger water exhauster: (a) Schematic of the equipment; (b) Conceptual model. Inspired by Romero et al.¹⁵

162 shown in Figure 3b, the compartment (1) represents the bottom section of the water exhauster with the
 163 exit streams being the enhanced regenerated TEG (L_1) and the vapor (V_1) flowing towards the top of
 164 the water exhauster. In the proposed model, the streams L_1 and V_1 are assumed to be in equilibrium.
 165 The overall composition of the compartment (1) is determined by the constant injection of stripping gas
 166 (G_0), the liquid stream coming from the reboiler (L_0), as well as by the internal vapor recirculation
 167 (V_{2R}) discussed below. The compartment (2) represents the top section of the water exhauster. It
 168 receives the vapor from the bottom section (V_1), which is partially condensed on the surface of the
 169 cooling tube bundle and removed from the vessel. The two streams leaving the compartment (2) are the
 170 condensate (L_2) and a vapor stream (V_2) representing the cooled, but uncondensed, vapor on the
 171 surface of the cold fingers. The streams L_2 and V_2 are assumed to be in equilibrium. The
 172 conceptualization represents the natural recirculation inside the vessel by the continuous reflux of a
 173 certain amount of uncondensed vapor coming from the second compartment and flowing back to the
 174 first one (V_{2R}). The condensate from the Coldfinger (L_2) is recycled to the still column, while the
 175 uncondensed vapor that is not recirculated to the bottom (V_{2S}) leaves the water exhauster from the top.
 176 In line with this conceptual model, two key variables are here introduced in order to represent the
 177 operating conditions of the Coldfinger water exhauster: (i) the internal recirculation of the vapor (α),
 178 defined as (V_{2R}/V_2) ; and (ii) the gas-to-liquid feed ratio (β), given by (G_0/L_0) .
 179 Based on this conceptualization, the Coldfinger water exhauster was modeled using Aspen HYSYS®
 180 V9.0 as shown in Figure 4. From a thermodynamic standpoint, the phase equilibrium conditions in the

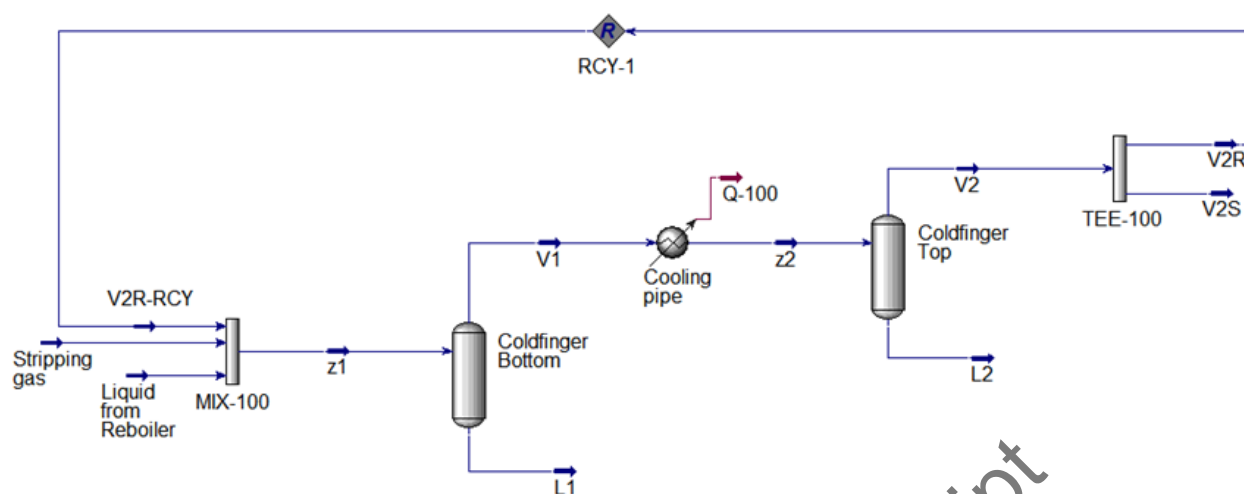


Figure 4. Conceptual model of the Coldfinger water-exhauster, as realized in Aspen HYSYS® V9.0.

compartment (1) (Coldfinger Bottom) were determined by means of PH-Flash calculations, assuming the compartment (1) to be adiabatic and the overall composition and the enthalpy of the system being thus determined by the inlet streams (the liquid feed from the reboiler, the stripping gas and the recirculation vapor). With regard to the top section of the Coldfinger (Coldfinger Top), i.e. the compartment (2), the analysis was carried out by fixing the top temperature (T_2), i.e. carrying out PT-Flash calculations. The top temperature was varied within the bottom temperature (maximum value) and values ensuring at least 5 °C of difference between T_2 and the exit temperature of the coolant flowing inside the cold fingers. Results not respecting this minimum temperature difference were discarded as considered technically unfeasible.

As regards the choice of the thermodynamic model, the literature shows that a number of models have been applied to simulate the fluid systems of interest in natural gas dehydration processes using TEG. These models include both cubic equations of state and activity coefficient models, as well as their

combinations (e.g. Twu-Sim-Tassone¹⁶ (TST), Peng-Robinson¹⁷, Cubic-Plus Association^{18,19} (CPA), NRTL,¹⁰ UMR-PRU²⁰). In this work, the Glycol property package of Aspen HYSYS[®] V9.0 was selected. It is based on the TST equation of state, and it was explicitly developed to accurately represent the TEG–water binary mixture and model gas dehydration units with TEG. The TST equation of state contains the necessary binary interaction parameters for the typical components encountered in a natural gas dehydration process, and its use is widespread among practitioners dealing with natural gas dehydration using TEG.

The present study is structured in two parts. In the first part, the behavior of the Coldfinger water exhauster as a standalone process unit is extensively analyzed, determining the effect of the key parameters (i.e. internal vapor recirculation, gas-to-liquid feed ratio, heat removal, temperature of the top section) on the level of enhanced TEG regeneration and highlighting key aspects of the functioning of the equipment. In the second part of the study, the water-exhauster model is included in process simulation schemes of complete gas dehydration units using Coldfinger for the glycol regeneration process. The results obtained with the proposed model are then compared with the data available in the literature referring to real plants.^{12,13}

3. Results and Discussion

3.1 Analysis of the Coldfinger Water Exhauster

In the analysis of the Coldfinger water exhauster as a standalone unit, the liquid feed was considered as a binary system (TEG + water) at saturation at 204 °C and 1.0 atm and its composition, calculated with the Glycol package, resulted to be: TEG 99.11 wt %; water 0.89 wt %. The selected values for pressure and temperature are representative of typical operating conditions of the reboiler of the still column. The composition of the stripping gas (G_0) entering the bottom section of the water exhauster is given as mole fractions in the following: methane 66.90 %; ethane 13.05 %; propane 12.20 %; i-butane 1.79 %; n-butane 3.97 %; i-pentane 0.48 %; n-pentane 0.45 %; n-hexane 0.08 %; carbon dioxide 0.11 %; nitrogen 0.97 %. This composition was selected as representative of a typical composition of dry gas, which was assumed to be available in the gas dehydration plant. The very small amount of water contained in the dry gas (mole fraction between $8.4 \cdot 10^{-5}$ and $1.5 \cdot 10^{-4}$, see Section 1) was neglected owing to the small gas flow rates characterizing the Coldfinger water exhauster, which make the mass of water in this stream several orders of magnitude lower than the mass of water contained in the liquid feed coming from the reboiler. TEG was selected as coolant of the compartment (2) with a flow rate equal to the one of TEG coming from the reboiler (i.e. the liquid feed) and an entry temperature in the heat exchanger pipes equal to approximately 40 °C. These choices are in line with the typical process design of the Coldfinger units for TEG regeneration, where the wet TEG exiting the absorber is used to cool the top section of the Coldfinger water exhauster. In the following analysis, the abovementioned parameter related to the stripping gas (β) is mass-based and the specific heat removed (Q) from compartment (2) is expressed taking 1 kg of liquid feed (L_0) as the basis of calculation. Using the model shown in Figure 4, a parametric study was created in which the following parameters were

varied: α , β and T_2 . For the parameter variation, the parameters α and β were expressed in a functional form, with an underlying exponent being parametrized: $\alpha = 1 - 10^a$; $\beta = 10^b$. The exponents a and b were varied between the lower and the upper bound with certain step sizes, as reported in Table 1. The temperature of the top compartment, i.e. T_2 , was varied between 200 °C (i.e. temperature approximately the same as the bottom compartment) and 50 °C with a step size of 10 °C. The lower bound value for T_2 is deemed a reasonable minimum value in a plant using the same circulating TEG as coolant. The ranges for the parameters are summarized in Table 1. A full factorial computer experiment was performed probing all possible combinations of the three parameters, giving a total of 2304 combinations. The parametric study was conducted using the Case Study tool built into Aspen HYSYS® V9.0. The results were exported, and data representation and visualization were performed in python using Numpy,^{21,22} Pandas²³ and Matplotlib.²⁴ Figures 5-7 show the TEG purity achieved in the water exhauster (stream L_1) as a function of the internal recirculation of the uncondensed vapor (α) for different values of the top temperature T_2 . Each figure refers to a fixed value of the gas-to-liquid feed ratio (β) with this parameter varied from 0.0001

Table 1. Ranges of the parameters applied in the Coldfinger parametric study.

Parameter	Lower bound	Upper bound	Step size	Steps
α : exponent, a	-3 ($\alpha = 0.999$)	0 ($\alpha = 0$)	0.20	16
β : exponent, b	-4 ($\beta = 0.0001$)	-2 ($\beta = 0.01$)	0.25	9
T_2	50 °C	200 °C	10 °C	16

to 0.01. The upper limit of the range set for β represents the typical stripping gas rate applied in a stripping gas TEG regeneration process.¹ Some of the curves stop at certain α values indicating that higher α values are not permissible according to the criterion based on the minimum temperature difference stated in Section 2. The values of TEG purity for $\alpha = 0$, i.e. absence of internal recirculation, correspond to the TEG enhanced purity that can be obtained by a conventional single-stage gas stripping operation. As a matter of fact, in the absence of internal recirculation, the compartments (1) and (2) are disconnected, and the mass fraction of TEG is simply raised owing to the application of the stripping gas in the compartment (1). Therefore, as expected, in the case $\alpha = 0$ the purity of TEG increases with β . The values range from 99.16 wt % ($\beta = 0.0001$, Figure 5) to 99.58 wt % ($\beta = 0.01$, Figure 7).

For $\alpha > 0$, Figures 5-7 show that the behavior of the Coldfinger water exhauster is non-obvious with operating regions allowing enhanced TEG purification compared to the single-stage gas stripping ($\alpha = 0$) but also operating regions leading to decreased TEG purity. In order to quantify this aspect, the Coldfinger Effect (CE) is here defined as

$$CE = \omega_{TEG,L_1}(\alpha, \beta) - \omega_{TEG,L_1}(\alpha = 0, \beta) \quad (1)$$

where: $\omega_{TEG,L_1}(\alpha, \beta)$ is the mass fraction of TEG attained by the water exhauster (stream L_1) in the presence of a certain internal recirculation of vapor ($\alpha > 0$) and a certain gas-to-liquid feed ratio (β); $\omega_{TEG,L_1}(\alpha = 0, \beta)$ is the mass fraction of TEG attained by the water exhauster (stream L_1) in the absence of internal recirculation ($\alpha = 0$) and for the same gas-to-liquid feed ratio (β).

Figures 5-7 show that a remarkable increase in TEG purity can actually be achieved with mass fractions up to almost 99.7 wt %, which cannot be obtained with the simple single-stage gas stripping

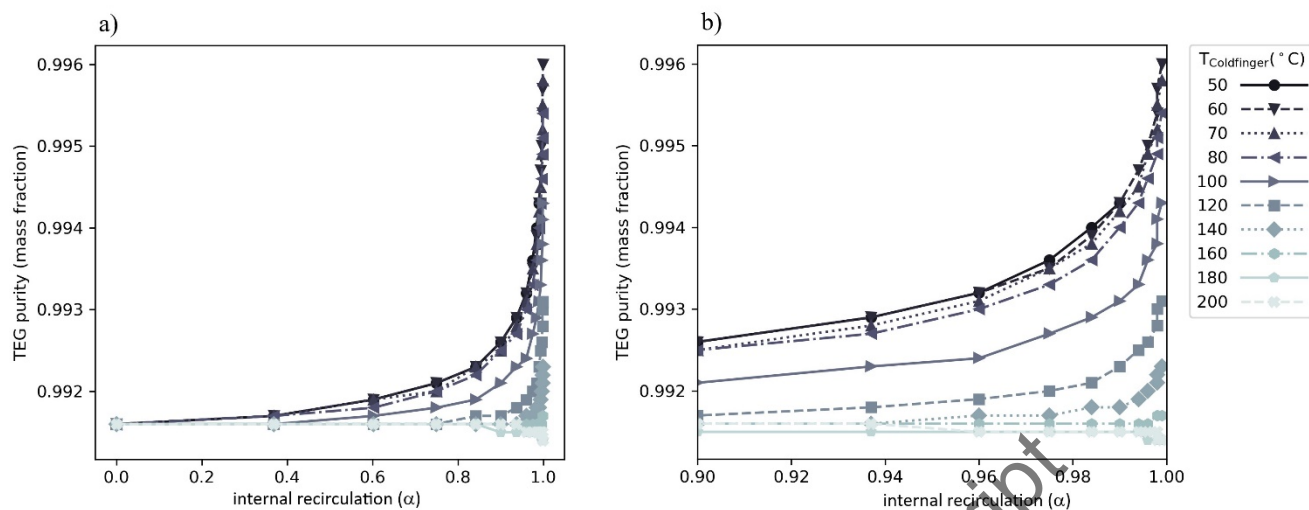


Figure 5. TEG purity at the exit of the water exhauster (stream L_1) as a function of the internal recirculation (α), for different values of the temperature at the top section of the Coldfinger (T_2). Gas-to-liquid ratio (β) equal to 0.0001. (a) Full range of α values; (b) α values between 0.90 and 1.0.

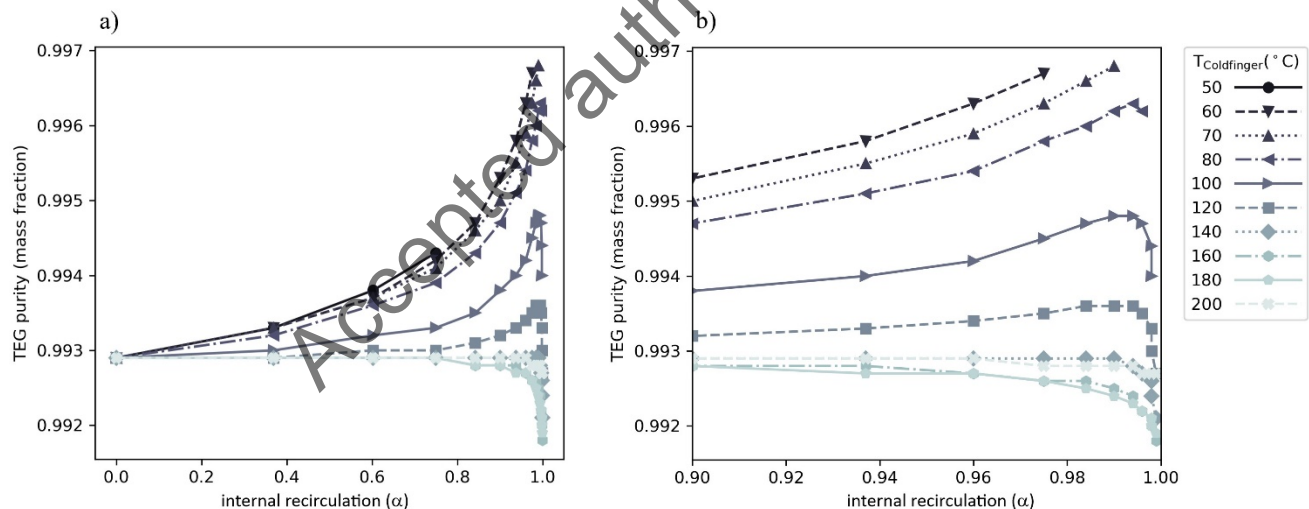


Figure 6. TEG purity at the exit of the water exhauster (stream L_1) as a function of the internal recirculation (α), for different values of temperature at the top section of the Coldfinger (T_2). Gas-to-liquid ratio (β) equal to 0.001. (a) Full range of α values; (b) α values between 0.90 and 1.0.

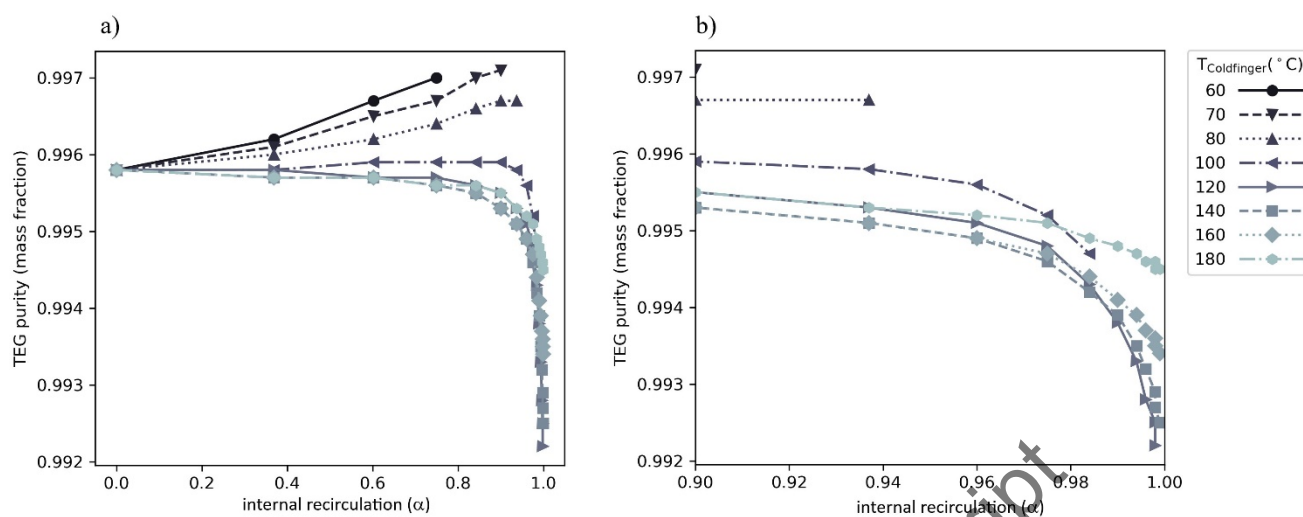


Figure 7. TEG purity at the exit of the water exhauster (stream L_1) as a function of the internal recirculation (α), for different values of the temperature at the top section of the Coldfinger (T_2). Gas-to-liquid ratio (β) equal to 0.01. (a) Full range of α values; (b) α values between 0.90 and 1.

In further detail, the perusal of Figures 5-7 shows the following patterns: (i) if the top temperature (T_2) is not sufficiently decreased, negative CE values are observed (i.e. Coldfinger water exhauster performing worse than the single-stage gas stripping unit for the same amount of gas fed to the equipment); (ii) below certain threshold T_2 values, the TEG purity increases with the internal recirculation (α), even though maximum points are observed in some cases; (iii) the threshold T_2 values decrease with β (i.e. higher stripping gas rates require lower temperatures at the top section); (iv) the maxima in TEG purity shift towards higher α values as β decreases; and (v) in all cases, TEG purities exceeding 99.6 wt % are observed, but the largest positive CE values are obtained for β values close to zero, α values close to one and top temperatures in the range of 50 to 80 °C. The latter point highlights that if relatively large amounts of stripping gas are used (e.g. $\beta = 0.01$),

300 the enhanced purity of TEG is basically caused by the stripping gas itself, similarly to a conventional
301 single-stage gas-stripping unit, making the possibility for additional purity induced by the Coldfinger
302 minimal. Moreover, if high levels of β are coupled with high values of α , the overall effect is even
303 worse than a conventional single-stage gas stripping unit. On the other hand, operations with extremely
304 small amounts of stripping gas (e.g. $\beta = 0.0001$) allow the same enhancement of TEG purity (up to
305 approximately 99.6 wt %) to be obtained as in a single-stage gas-stripping unit but consuming by far
306 less gas (in the order of 10 – 100 times less). In this case, the TEG enhanced purity is basically caused
307 by the Coldfinger mechanism, rather than the action of the stripping gas itself. Overall, it can be stated
308 that the proper working range of the Coldfinger water exhauster is at very high α (at least 0.95) and
309 very low β (not higher than 0.001).

310 Another perspective on the behavior of the Coldfinger can be obtained by analyzing the performance of
311 the water exhauster as a function of the heat removed from the vapor section. In this regard, Figures 8-9
312 depict the trends of the attained TEG mass fraction (in the stream L_1) as a function of the specific heat
313 removed, for α equal to 0.960 and 0.999, respectively, and varying β within the range of the study.
314 Both figures show the presence of operating regions where the TEG purity increases with the heat
315 removal, but also operating regions where the opposite occurs. Considering the curves at lower β
316 values in Figure 8, starting from null heat removal and increasing it, there is an initial region where the
317 TEG purity is roughly constant or slightly decreasing. Further increasing the heat removal, there is a
318 region characterized by a steep increase of the TEG purity followed by a change of concavity
319 indicating that further heat removal becomes progressively less effective. The curves at the higher β
320 values, instead, show a very large operating region where the TEG purity decreases, with this trend
321 being reversed only for very high levels of heat removal. It is noted that the curves stop where the heat

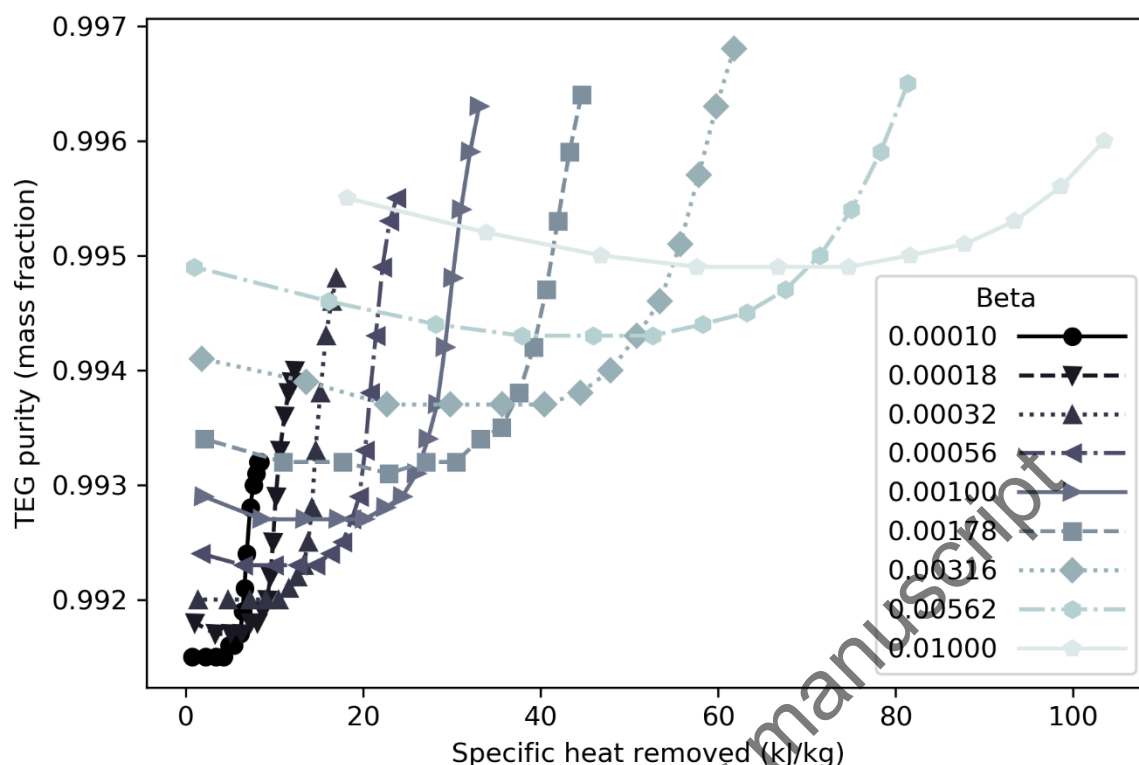


Figure 8. TEG mass fraction at the exit of the water exhauster (stream L_1) as a function of the specific heat removed from the vapor section of the Coldfinger, for different values of gas-to-liquid ratio (β). Internal recirculation (α) equal to 0.960. The specific heat is the ratio of the heat rate removed in the top section to the mass flow rate of the stream L_0 .

removed could not be further increased due to the constraint imposed at the heat exchanger in the compartment (2), as discussed in Section 2.

As can be seen from Figure 9, the difference between the trends of the curves at different values of β becomes even more dramatic at very high α (i.e. 0.999). It can be noted that TEG purities above 99.5 wt % can be attained with β values around 0.0001 – 0.0003, while comparable levels of TEG purity are

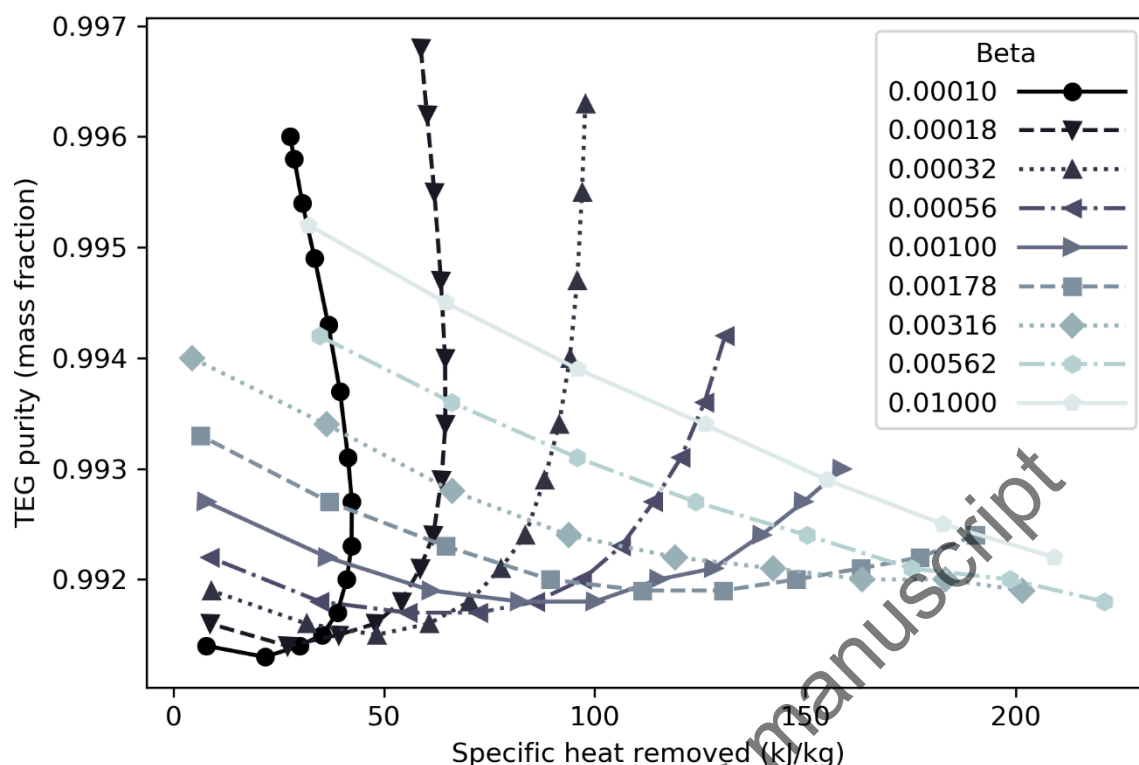


Figure 9. TEG mass fraction at the exit of the water exhauster (stream L_1) as a function of the specific heat removed from the vapor section of the Coldfinger, for different values of gas-to-liquid ratio (β). Internal recirculation (α) equal to 0.999. The specific heat is the ratio of the heat rate removed in the top section to the mass flow rate of the stream L_0 .

also attained in a completely different operating region of the equipment, characterized by a gas-to-liquid ratio more than 30 times higher ($\beta = 0.01$). In the former case, it is basically the Coldfinger effect that is leading to the purification of TEG, while in the latter case the system behaves similarly to a conventional single-stage gas stripping unit. In this regard, it is worth noting that an isothermal single-stage gas stripping unit with $\beta = 0.01$ leads to TEG mass fraction of 99.58 wt % (see Figure 7,

for $\alpha = 0$), which means that a comparable TEG enrichment can be obtained by the Coldfinger water exhauster using approximately 30 to 100 times less gas.

Another peculiar phenomenon can be highlighted from Figure 9 with respect to the operating region at low β values (below approximately 0.0002), which is the most interesting region from the point of view of efficient Coldfinger operation. Multiple steady-states can be observed for given inlet conditions to the exhauster and given heat removal. For instance, considering a specific heat removed of about $30 \frac{kJ}{kg}$, for $\beta = 0.0001$ and $\alpha = 0.999$, the TEG purity at the exit of the water exhauster (stream L_1) can be as low as 99.14 wt % (case (a)) or as high as 99.54 wt % (case (b)) for same input streams and (basically the same) heat removal on top. The analysis of the simulation output comparing the low-efficiency case (a) for heat removal of $29.97 \frac{kJ}{kg}$ and the high-efficiency case (b) of similar heat removal (i.e. $30.63 \frac{kJ}{kg}$) shows that: (i) the mass flow rate of the stream V_1 (relative to L_0) in case (a) is 0.27, which is approximately six times higher than in case (b), where it is 0.045; (ii) the total mass fraction of water and TEG in said stream is 79.6 wt % in case (a), while it is 59.5 wt % in case (b), the rest being essentially non-condensable gases; (iii) the mass fraction of water in said stream is 47.0 wt % in case (a), while it is 25.3 wt % in case (b); and (iv) the top temperature (T_2) is 180 °C in case (a) while it is 80 °C in case (b). When this stream is cooled down in the compartment (2), in case (a) the fraction condensed ($f_L = \frac{L_2}{V_1}$) is only 0.16 with the liquid stream L_2 being 98.74 wt % TEG and 1.25 wt % water (TEG/water ratio equal to 79 on mass basis). On the other hand, in case (b) a higher fraction condensed is achieved (i.e. $f_L = 0.44$) with a mass fraction of TEG of 77.7 wt % and a mass fraction of water of 22.3 wt % (TEG/water ratio equal to 3.5 on mass basis). Therefore, in case (a) (low efficiency) the large mass flow rate of V_1 does not allow a substantial temperature reduction on the top of the

365 equipment (for the same heat) and most of the latent heat is actually used for condensing TEG, i.e. the
366 heaviest component, rather than water. This leads to a large amount of internally circulating streams,
367 with water mostly recirculating inside the system. On the other hand, in case (b) (high efficiency, i.e.
368 high Coldfinger Effect) the mass flow rate of V_1 is much lower, and the same amount of removed heat
369 is efficiently used to condense and remove water, besides TEG, in conjunction with a larger amount of
370 internal recirculation of non-condensables and lower top temperature.

371 This behavior is highlighted in Figure 10, which shows the water removal ratio in the top compartment
372 (mass flow rate of water in the stream L_2 divided by the mass flow rate of water in V_1). As can be seen,
373 the water removal ratio in compartment (2) varies dramatically with the operating region of the water
374 exhauster. At large β values, the heat removal is not effective, as it cannot be enough to promote
375 substantial water condensation and removal. Under these conditions, the system behaves similarly as a
376 conventional single-stage stripping section and may also lead to worse results compared to it. At lower
377 β values, there are operating regions that can lead to very high water removal ratios. These operating
378 regions allow attaining high Coldfinger Effect values.

379

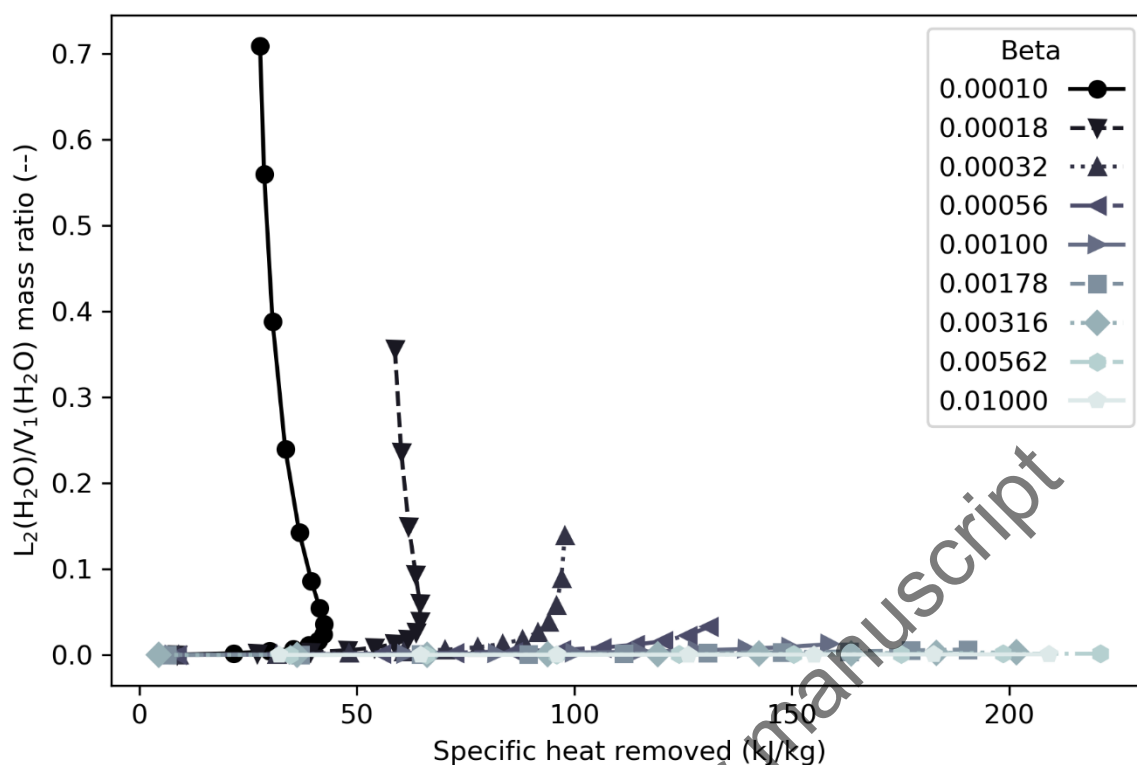


Figure 10. Water removal ratio in the compartment (2), i.e. the top section of the Coldfinger, as a function of the specific heat removed, for $\alpha = 0.999$ and different β values.

3.2 Comparison and Validation Against Plant Data

3.2.1. Coldfinger Patent Analysis

Process data was sourced from patent number 4,332,643 of Reid¹² in order to validate the conceptual model shown in Figure 4 extracting the information needed to apply the Coldfinger conceptual model. In the first embodiment of the invention, various data is provided according to a process configuration basically the same as the one reported in Figure 2. In particular, rich glycol from the absorber is used to remove heat from the top section of the water exhauster. In the body of the text of the detailed description, what is perceived as “typical” performance data was referenced. In addition, a table with so-called “sample source” data is provided, which is conceived as being an example of real plant data. The conceptual model described in Section 2 was thus used to emulate both the “typical” and the “sample source” data provided in the patent.¹²

With regard to the “typical” data, the mass flow rate of the liquid feed to the water exhauster (L_0) was fixed as in the patent data at 3727 kg/h. The inlet temperature of the stream L_0 was calculated in order to match the given TEG mass fraction of said stream (99.0 wt %). The calculated value (201.7 °C) is within the typical range as reported in the patent¹² (199 to 221 °C). The specific heat removal of the “typical” data was estimated from the temperature values of the rich glycol at the inlet (48.9 °C) and the outlet (54.4 °C) of the Coldfinger heat exchanger using an average constant-pressure heat capacity of $3.2 \frac{\text{kJ}}{\text{kg K}}$. A value of $18 \frac{\text{kJ}}{\text{kg}}$ was found (taking L_0 as basis of calculation). It is noted that these temperatures in the patent are referred to as approximate. As discussed in Section 2, the conceptual model is based on three parameters: α , β , and T_2 . α is constrained between 0 and 1, β has a lower bound of 0, and T_2 depends on the Coldfinger heat exchanger design and performance, such as heat transfer

411 surface area, cooling medium temperature, etc. Using the built-in optimizer in the process simulator
412 employing Sequential Quadratic Programming (SQP/SLSQP),²⁵ an objective function is formulated for
413 the optimizer to find the values of α , β and T_2 giving the best match. The problem is formulated as a
414 least-squares problem of the difference between the following plant and simulated data: (i) TEG purity
415 in the stream L_1 ; (ii) Coldfinger condensate rate (L_2); (iii) temperature increase on the tube side of the
416 Coldfinger heat exchanger. With respect to the latter point, the energy balance at the Coldfinger heat
417 exchanger was included in the least squares formulation. The full results of the optimization are
418 presented in the Supporting Information (Table S1), while the main results are summarized in the
419 following.

420 The conceptual model is able to provide a very good match for the “typical” data case. The achieved
421 TEG purity is matched (simulated value: 99.5 wt %; plant data: 99.6 wt %) within typical uncertainties
422 of experimental measurements of water-in-TEG at high dilution (e.g. Karl-Fischer titration) as well as
423 within typical uncertainties of thermodynamic model predictions in this high-dilution region. It is
424 important to observe that the optimal match is achieved for $\alpha = 0.995$ and $\beta = 1.2 \cdot 10^{-4}$, which are
425 values corresponding to high CE values as discussed in Section 3.1. The moderate discrepancies in the
426 specific heat removal (simulated: 22.7 kJ/kg; plant data: 18 kJ/kg) and in the mass flow rate of
427 condensate (L_2) at the Coldfinger (simulated: 51 kJ/kg; plant data: 44 kJ/kg) appear to be in line with
428 the tube-side temperature differences of the rich glycol defined as approximate in the patent
429 description.¹² The discrepancy in the exit temperature of dry TEG (simulated: 197 °C; plant data: 177-
430 182 °C) is probably due to the absence of heat losses in the simulations compared to “typical” plant
431 operation. The glycol/water ratio in V_1 (1.19) is within the broad range considered as typical (0.54 to

1.44). Overall, the results are substantially in line with both the patent description and the conceptual model results presented in Section 3.1.

A similar optimization approach was also carried out for the so-called “sample source”, which provides a different type of data set. Specifically, the feed data are provided, including the mass fraction of TEG (99.1 wt %) and the temperature (201.7 °C). The feed flow rate is provided in volumetric terms and was therefore converted into mass basis, assuming the density of TEG to be 1.13 kg/m³, giving ($L_0 = 2046 \frac{kg}{h}$). In addition, the temperature of the dry TEG at the exit of the water exhauster is also given (176.7 °C), as well as the composition of the water exhauster condensate, which is to be discussed below. However, in this case the patent data include neither the heat removal rate nor the condensate rate. In line with the available information, the formulation of the least-squares problem was set to minimize the discrepancy between the purity and the temperature of TEG in L_1 . In addition, the energy balance at the Coldfinger heat exchanger was included in the problem formulation to ensure that the difference between the temperature of V_1 and the TEG (coming from the absorber and used for cooling) leaving the heat exchanger had a positive value.

The model is able to yield an almost perfect match with respect to both the achievable TEG purity (simulated 99.7 wt %; plant data 99.7 wt %) and the temperature of the concentrated TEG leaving the water exhauster (simulated 176.4 °C; plant data 176.7 °C). It is worth noting that in this case there is one degree of freedom, as the minimization of two parameters is based on three optimization variables (α , β and T_2), meaning that there could potentially be a manifold of combinations of α , β and T_2 that could provide equally good matches to the data. However, the TEG purity is close to the maximum achievable, which limits the parametric space. Furthermore, it is important to observe that the

453 combination of α , β and T_2 values minimizing the discrepancies is again located in the characteristic
454 region of efficient Coldfinger operation (i.e. high CE values) with values being in line with the
455 theoretical description and considerations of Section 3.1: $\alpha = 0.999$; $\beta = 3.3 \cdot 10^{-4}$; and $T_2 = 69^\circ\text{C}$.
456 A large discrepancy is observed on the TEG mass fraction in the condensate (L_2), which is reported as
457 46 wt % in the plant data while the simulated value is 87 wt %. This appears to be an outlier compared
458 to the other parameters. However, it is noted that the simulated mass fraction (87 wt %) corresponds to
459 a mole fraction of 45 %. Even though all compositional data in the sample source are stated as being on
460 mass basis, it is considered likely that this is a typographical error in the patent, considering the fact
461 that all other main parameters exhibit a very good match. Compared to the “typical” data, it is seen
462 that, in order to match the “sample source” data, a somewhat higher β and a much higher value of
463 specific heat removed (94.9 kJ/kg) are needed. As can be seen from Figure 9, the need for higher heat
464 removal with a higher β is consistent, if a high TEG purity is to be achieved. From a practical
465 standpoint, this high value of heat removal seems to be possible only due to a very cold (i.e. 13°C)
466 diluted TEG used as cooling medium in the Coldfinger tube side according to the patent. For most
467 applications, such a low temperature is not considered practical, and the achieved TEG purity appears
468 to be optimistic. The complete set of data pertaining the “sample source” case is reported in the
469 Supporting Information (Table S2).

470 Overall, the proposed model is able to reproduce the key values of the Coldfinger patent by Reid¹² with
471 the optimal values of the regression parameters bearing physical meaning according to the theoretical
472 analysis of Section 2 and the related data of Section 3.1. The simulations of the patent data further
473 confirm that the Coldfinger functionality is able to provide a positive effect on the TEG purity
474 increasing it from around 99.0 wt % – 99.1 wt % to 99.5 wt % – 99.7 wt % using minimal source of

external gas. In this study, the gas is referred to as stripping gas, as in the simulation it is used as a continuous-flow of dry gas in the same fashion as in the conventional TEG enhanced regeneration stripping gas process. However, the amount of gas needed in the Coldfinger process is substantially lower, i.e. up to two orders of magnitude. From a practical standpoint, this means that the gas can be provided by any source of gas available in very small amounts in a processing plant, such as e.g. nitrogen used as inert medium.

3.2.2. Domestic gas processing plant analysis

The following sub-sections focus on the application of the Coldfinger model presented in this work on the plant data provided by Rahimpour et al.¹³ In Section 3.2.2.1, the Coldfinger model is embedded in a full process simulation scheme and used to emulate the plant data reported by Rahimpour et al.¹³ In Section 3.2.2.2, it is shown how the plant operation reported by Rahimpour et al.¹³ could be optimized based on the optimal selection of the process parameters characterizing the Coldfinger model.

To the best of the authors' knowledge, except for the data provided in the Reid's patent¹² investigated in the previous section, the only Coldfinger plant data available in the literature are those reported in the work by Rahimpour et al.¹³ In addition, neither laboratory or pilot plant data are known.

3.2.2.1. Process simulation

The process scheme of the domestic gas plant, as presented in the work by Rahimpour et al.,¹³ is shown in Figure 11. Operating conditions of the plant are taken from Tables 4-6 of the work of Rahimpour et

al.¹³ It is a plant treating 513 t/h of wet gas, available at 69 bar and 40 °C (Stream 1). Indicating the composition as mole fractions, the gas is composed of methane (85 %) and ethane (5.5 %), with C3 – C5 around 3.5 %, the rest essentially being heavier hydrocarbons (0.7 %), nitrogen (3.5 %), CO₂ (1.3 %), water (0.14 %) and impurities. Lean TEG at 45.0 °C is fed at the top of the absorption column (Stream 16) with a mass flow rate of 15.3 t/h. The rich TEG exiting the bottom of the column, operated at 69 bar, is expanded to 8.8 bar and conveyed to the tube side of the Coldfinger heat exchanger (Stream 6). At the exit (Stream 7), the temperature of TEG is increased by 8.3 °C. The number of theoretical stages of the absorber (N_A) is not provided. Typical values are in the range of

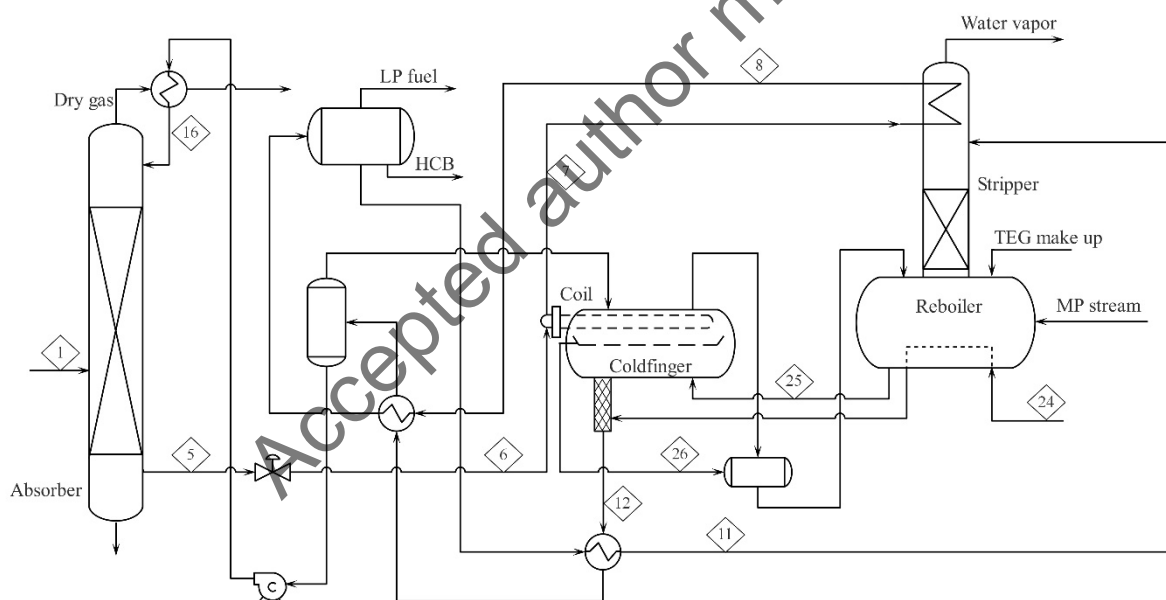


Figure 11. Domestic gas processing plant with Coldfinger. Based on the information available in Rahimpour et al.¹³ and redrawn focusing on the essential process aspects only.

1 to 3.¹ Preliminary simulations showed that the dry gas composition reported in the plant data¹³ was in between simulation results obtained for two and three theoretical stages. $N_A = 3$ was assumed. The rich TEG is further heated in the condenser at the top of the regeneration column and in a recovery heat exchanger prior to be flashed at 5.8 bar and 82.0 °C. The rich TEG exiting the flash drum is conveyed to an additional recovery heat exchanger and then fed to the regeneration column. The number of theoretical stages of the regeneration column is not provided. In the process simulations, it was assumed to be equal to three, as this is also a typical value. The reboiler of the column is operated at 207 °C. The pressure at the top of the column is reported to be 1.16 bar. Assuming the reboiler and the water exhauster to operate at basically the same pressure, the value is set to 1.28 bar for both in order to match the plant data of the pressure value of the gas stream flashed off from lean TEG and recycled to the Coldfinger water exhauster. A part of the dry gas (206.2 kg/h) produced in the absorber is heated in the reboiler (Stream 24) and used as stripping gas by feeding it to a small packed column placed below the water exhauster, and then it enters the Coldfinger apparatus. Details on the packing column are not provided. The packed column is assumed to be equivalent to two theoretical stages. The abovementioned data were taken as input data in the process simulations, in which the Coldfinger water exhauster model was embedded. In particular, it is noted that the tube-side temperature variation in the Coldfinger heat exchanger was fixed as per the plant data in order to ensure (approximately) the same heat removal in the top compartment of the water exhauster. This left only one degree of freedom for the analysis of the Coldfinger model, i.e. the internal recirculation of vapor (α), which was varied to attain the best match with the TEG purity of Stream 12.

A very good match with the plant data is achieved, with the best match obtained with $\alpha = 0.89$. In particular, the mass fraction of enriched TEG (Stream 12) was found to be 99.64 wt %, which matches

perfectly the composition on a (TEG+water) basis (simulated 99.7 wt %; plant data 99.7 wt %). This is obtained with a TEG exit temperature close to the plant data (simulated 193.7 °C; plant data 196 °C), as well as with approximately the same specific heat removal in the top compartment (simulated 25.42 kJ/kg; plant data 25.33 kJ/kg). The thermodynamic model applied in this work predicts 41 °C at the exit of the absorber (Stream 41) and a slight temperature increase in the valve expansion yielding to 42.6 °C in Stream 6. The temperatures of both Stream 5 and Stream 6 in the plant data are given as 40.5 °C. It is remarked that, in the simulation of this work, the same temperature difference between Stream 7 and Stream 6 was imposed, in order to match, as a good approximation, the heat removal in the top compartment of the Coldfinger. Overall, the model proposed in this work allows some flexibility via the internal recirculation parameter (α), to match typical plant data while bearing a sound physical meaning. Key simulation outputs are reported in the Supporting Information (Table S3).

It is noted that the gas flow rate applied in the plant corresponds to a gas-to-liquid feed ratio (β) around 0.013. According to the analysis of Section 3.1, the operating regime of the Coldfinger water exhauster for such high β values is characterized by low or even negative values of CE with the TEG enrichment being mainly due to the conventional gas stripping itself.

3.2.2.2. Process optimization

As apparent from the process analysis of Sections 3.1 and 3.2.2.1, the operating parameters presented in the paper of Rahimpour et al.¹³ refer to a water exhauster that is basically working as a conventional gas stripping unit, which is to say without exploiting the specific and intended features of the Coldfinger water exhauster. In order to verify the possibility of achieving comparable levels of TEG

550 dehydration by operating the Coldfinger water exhauster with substantially less stripping gas, an
551 optimization study was carried out. For that purpose, the key Coldfinger model parameters (α , β , and
552 T_2) were varied, for other input parameters as in Section 3.2.2.1 being the same (except the tube-side
553 temperature difference of TEG used as a coolant), to determine better operational conditions. This
554 optimization scenario corresponds to a theoretical maximum of TEG purity obtainable for the studied
555 domestic gas processing plant, according to the model presented in this work, without placing
556 limitations on the heat exchanger in the Coldfinger top section. Furthermore, the assessment considered
557 the proper working range of the Coldfinger water exhauster (Section 3.1) at α close to one, β close to
558 zero and top temperatures in the range of 50 to 70 °C.

559 The highest TEG enhanced purity found was 99.65 wt %, with a top section temperature of 60 °C,
560 equivalent to a specific heat removal of 58 kJ/kg, α equal to 0.999 and β equal to 3.16×10^{-4} ,
561 equivalent to 5 kg/h of stripping gas. Figure 12 depicts the correlation of the key parameters assessed to
562 find the operational range. As observed, the higher values of TEG enhanced purity were found for the
563 highest values of α and β from the range analyzed. The optimal conditions show that approximately
564 the same TEG enrichment (99.63 wt %) can be obtained with significantly lower amounts of stripping
565 gas (5 kg/h instead of 206 kg/h) by operating the Coldfinger water exhauster in a different region,

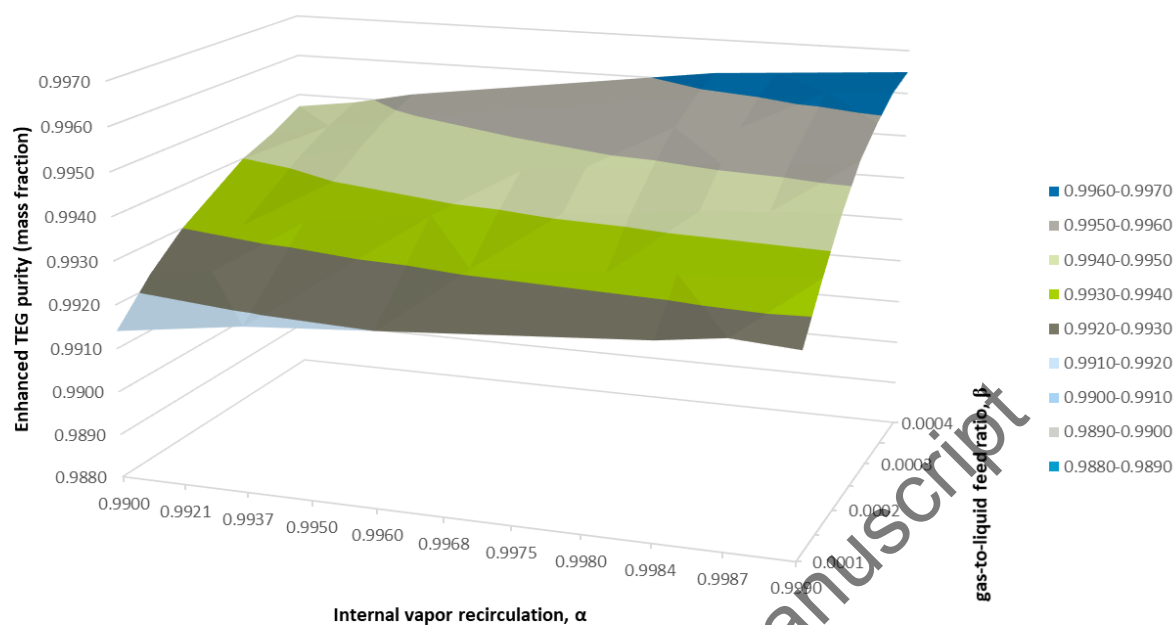


Figure 12. Enhanced TEG purity as a function of α and β at top temperature of 60 °C.

basically characterized by: (i) lower gas injection; (ii) higher gas internal recirculation; (iii) larger heat removal.

The present analysis clearly shows that while the injection of stripping gas is in general considered beneficial in order to obtain higher purities in advanced TEG regeneration, if coupled with a Coldfinger water exhauster, it can actually decrease CE , making the Coldfinger itself redundant, or it can even revert CE to negative values, i.e. it can lead to lower TEG enrichment compared to the case of a conventional single-stage gas stripping unit, for the same amount of gas.

However, it is also shown that the same Coldfinger unit, if subjected to a much lower stripping gas rate and a higher heat removal, has the possibility of functioning according to its design intent and can provide a TEG purity comparable to that obtained with a much higher stripping gas rate.

4. Conclusions

This work proves that a simple equilibrium-stage based model is able to reproduce the observed plant data of the Coldfinger water exhauster for enhanced glycol regeneration in natural gas dehydration plants. The model represents the Coldfinger water exhauster as a two-stage equilibrium unit with internal recirculation of uncondensed top vapor. The model is easy to implement in commercial process simulators and can be embedded in full simulation schemes of natural gas dehydration using glycols.

The significance of key model parameters (internal vapor recirculation α ; gas-to-liquid feed ratio β ; top section temperature T_2) and their interactions are highlighted. The results of the study of the Coldfinger as a standalone unit (Section 3.1) illustrate that the Coldfinger water exhauster is most effective when the top section is cooled down to 50 to 80 °C with internal recirculation of uncondensed vapor approaching one (above 0.95) and very low values of gas fed to the system (gas-to-liquid ratios in the order of 10^{-4}). The model indicates that TEG purities of up to 99.7 % are achievable. The concept of the Coldfinger Effect (CE) is introduced in this work, representing the additional TEG dehydration generated by the Coldfinger water exhauster with respect to a conventional single-stage gas stripping unit utilizing the same amount of gas. The largest positive values of CE are seen for very low, yet positive, values of gas fed to the exhauster (gas-to-liquid feed ratios in the order of 10^{-4}). Under proper operating conditions, the Coldfinger water exhauster is able to attain the same TEG purity levels as

597 conventional single-stage gas stripping units by using 10 to 100 times less gas. The analysis, however,
598 also shows that the behavior of the Coldfinger water exhauster is non-obvious. In particular, operating
599 regions characterized by negative CE are observed, as well as optimal internal recirculation values.
600 Furthermore, this work shows the possibility of two different steady-states compatible with given feeds
601 and given heat removals in the top section, with one steady-state being characterized by low-efficiency
602 and the other by high-efficiency. The observed non-obvious behaviors are explained in terms of the
603 efficient use of the heat removal, which is mainly determined by the top condensation. The same
604 amount of removed heat can yield to a high level of TEG condensation and a low level of water
605 condensation resulting in poor overall efficiency, or in a high level of water condensation and removal
606 resulting in a large CE .

607 The proposed conceptual model is validated against published plant data (Section 3.2) retrieved from a
608 Coldfinger patent¹² and from a recent paper.¹³ A good match is observed between the proposed model
609 and the available plant data, with model regression parameters attaining optimal values bearing
610 physical significance in line with the conceptualization provided in Section 3.1. This shows that the
611 model is able to capture the main effects leading to TEG enrichment by controlling a few key variables
612 of the Coldfinger water exhauster with a sound physical meaning. It is noted, however, that the internal
613 recirculation (α) is an empirical parameter, embedding mass transfer phenomena (such as those
614 generated by the natural convection inside the equipment) without an attempt of describing them in
615 detail. Further studies connecting the phase equilibrium based approach presented in this work with
616 natural convection and fluid dynamics aspects pertaining to the vapor internal circulation, as well as
617 with design aspects of the top heat exchanger, may provide further advancement in the insight into the
618 functioning of the Coldfinger water exhauster.

619 **Supporting information**

620 Comparison between simulation results of the Coldfinger water exhauster with the “typical” plant data
621 reported in the patent U.S. 4,332,643 of Reid¹² (Table S1).

622 Comparison between simulation results of the Coldfinger water exhauster with the “sample source”
623 plant data reported in the patent U.S. 4,332,643 of Reid¹² (Table S2).

624 Comparison between simulation results and data from domestic gas plant¹³ (Table S3).

625 This information is available free of charge via the Internet at <http://pubs.acs.org/>.

626

627 **Acknowledgments**

628 This work was not supported by any specific funding body.

Accepted author manuscript

References

- (1) GPSA Editorial Review Board. Gas Dehydration (Section 20). In *GPSA Engineering Databook*; GPSA: Tulsa, Oklahoma, 2012.
- (2) Kidnay, A. J.; Parrish, W. R.; McCartney, D. G. *Fundamentals of Natural Gas Processing, Third Edition*; CRC Press, 2019.
- (3) Kong, Z. Y.; Mahmoud, A.; Liu, S.; Sunarso, J. Revamping Existing Glycol Technologies in Natural Gas Dehydration to Improve the Purity and Absorption Efficiency; Available Methods and Recent Developments. *J. Nat. Gas Sci. Eng.* **2018**, *56*, 486.
- (4) Ghiasi, M. M.; Bahadori, A.; Zendehboudi, S.; Chatzis, I. Rigorous Models to Optimise Stripping Gas Rate in Natural Gas Dehydration Units. *Fuel* **2015**, *140*, 421.
- (5) Neagu, M.; Cursaru, D. L. Technical and Economic Evaluations of the Triethylene Glycol Regeneration Processes in Natural Gas Dehydration Plants. *J. Nat. Gas Sci. Eng.* **2017**, *37*, 327.
- (6) Kong, Z. Y.; Mahmoud, A.; Liu, S.; Sunarso, J. Development of a Techno-Economic Framework for Natural Gas Dehydration via Absorption Using Tri-Ethylene Glycol: A Comparative Study on Conventional and Stripping Gas Dehydration Processes. *J. Chem. Technol. Biotechnol.* **2019**, *94*, 955.
- (7) Saidi, M.; Parhouch, M.; Rahimpour, M.R. Mitigation of BTEX Emission from Gas Dehydration Unit by Application of Drizo Process: A Case Study in Farashband Gas Processing Plant; Iran. *J. Nat. Gas Sci. Eng.* **2014**, *19*, 32.
- (8) Kong, Z. Y.; Wee, X. J. M.; Mahmoud, A.; Yu, A.; Liu, S.; Sunarso, J. Development of a Techno-Economic Framework for Natural Gas Dehydration via Absorption Using Tri-Ethylene Glycol: A Comparative Study between DRIZO and Other Dehydration Processes. *S. Afr. J. Chem. Eng.* **2020**, *31*, 17.

- 652 (9) Gironi, F.; Maschietti, M.; Piemonte, V.; Diba, D.; Gallegati, S.; Schiavo, S. Triethylene Glycol
653 Regeneration in Natural Gas Dehydration Plants: A Study on the Coldfinger Process. Proceedings
654 of the 8th Offshore Mediterranean Conference and Exhibition (OMC 2007), Ravenna, March 28-
655 30, 2007.
- 656 (10) Piemonte, V.; Maschietti, M.; Gironi, F. A Triethylene Glycol-Water System: A Study of the TEG
657 Regeneration Processes in Natural Gas Dehydration Plants. *Energ. Source Part A* **2012**, 34, 456.
- 658 (11) Reid, L. S. Apparatus for Dehydrating Organic Liquids. US Patent 3589984, 1971.
- 659 (12) Reid, L. S. Method of Removing Water from Glycol Solutions. US Patent 4332643, 1982.
- 660 (13) Rahimpour, M. R.; Jokar, S. M.; Feyzi, P.; Asghari, R. Investigating the Performance of
661 Dehydration Unit with Coldfinger Technology in Gas Processing Plant. *J. Nat. Gas Sci. Eng.*
662 **2013**, 12, 1.
- 663 (14) Øi, L. E.; Selstø, E. T. Process Simulation of Glycol Regeneration. For presentation at GPA
664 Europe's Meeting, Bergen, Norway, 2002.
- 665 (15) Romero, I.A.; Andreasen, A.; Nielsen, R.; Maschietti, M. Modeling of the Coldfinger Water
666 Exhauster for Advanced TEG Regeneration in Natural Gas Dehydration. *Chem. Eng. Trans.* **2019**,
667 74, 661.
- 668 (16) Twu, C. H.; Tassone, V.; Sim, W. D.; Watanasiri, S. Advanced Equation of State Method for
669 Modeling TEG-Water for Glycol Gas Dehydration. *Fluid Phase Equil.* **2005**, 228–229, 213.
- 670 (17) Gironi, F.; Maschietti, M.; Piemonte, V. Natural Gas Dehydration: A Triethylene Glycol-Water
671 System Analysis. *Energ. Source Part A* **2010**, 32, 1861.
- 672 (18) Arya, A.; Maribo-Mogensen, B.; Tsivintzelis, I.; Kontogeorgis, G.M. Process Design of Industrial
673 Triethylene Glycol Processes Using the Cubic-Plus-Association (CPA) Equation of State. *Ind.*
674 *Eng. Chem. Res.* **2014**, 53, 11766.

- 675 (19) dos Santos, L. C.; Abunahman S. S.; Tavares, F. W.; Ahón, V. R. R.; Kontogeorgis, G.M. Cubic
676 Plus Association Equation of State for Flow Assurance Projects. *Ind. Eng. Chem. Res.* **2015**, *54*,
677 6812.
- 678 (20) Petropoulou, E. G.; Voutsas, E. C. Thermodynamic Modeling and Simulation of Natural Gas
679 Dehydration Using Triethylene Glycol with the UMR-PRU Model. *Ind. Eng. Chem. Res.* **2018**, *57*,
680 8584.
- 681 (21) Oliphant, T.E. *A Guide to NumPy*; Trelgol Publishing, USA, 2006.
- 682 (22) van der Walt, S.; Colbert, S. C.; Varoquaux, G. The NumPy Array: A Structure for Efficient
683 Numerical Computation. *Comput. Sci. Eng.* **2011**, *13*, 22.
- 684 (23) McKinney, W. Data Structures for Statistical Computing in Python, Proceedings of the 9th Python
685 in Science Conference (SCIPY 2010), **2010**, 56.
- 686 (24) Hunter, J.D. Matplotlib: A 2D Graphics Environment. *Comput. Sci. Eng.* **2007**, *9*, 90.
- 687 (25) Kraft, D. Algorithm 733: TOMP–Fortran Modules for Optimal Control Calculations. *ACM Trans.*
688 *Math. Softw.*, **1994**, *20*(3), 262.
- 689
- 690

